KTH Engineering Sciences

An Analysis of Residual Radiation in Thoriated Camera Lenses

Jonathan Wäng* and Viktor Henningsson†

*jonwan@kth.se, †vikhen@kth.se

SA104X Degree Project in Engineering Physics, First Level

Supervisor: Bo Cederwall

Department of Physics
School of Engineering Sciences
Royal Institute of Technology (KTH)

Stockholm, Sweden, 2013

Abstract

The usage of the naturally occurring radioactive isotope thorium-232 in older camera lenses was implemented to provide better optical properties and a cheaper production. In this thesis, the resulting radioactivity in camera objectives containing such lenses is studied via gamma spectroscopy. A number of camera objectives that potentially contain thorium-232 were measured using a germanium semiconductor photon detector. The spectra were compared to the background radiation whereby it is possible to determine whether any inherent radiation from the thorium-232 decay chain came from the lenses themselves. For one lens, the gamma spectra are then complemented with beta emission spectroscopy. From this, it is finally possible to establish the activity of the lenses and the radiation dose a photographer would receive from them. The radiation dose can then be compared to national standards of allowed doses. The measurements showed that though there clearly was a presence of decaying thorium and daughter nuclides in the objectives, the activity was small enough not to be hazardous.

Contents

1 Introduction

1.1 Background

Beginning in the end of the 1930's and up until sometime in the 1980's, thorium was sometimes used in the lenses of photographic objectives to improve their optical properties. Paul De Paolis at Kodak patented some specific formulae for optical glass with thorium in 1949 [1]. This could be an indicator of when commercial thoriated lenses were first sold. Thorium-232 was used, both blended in with the glass and as a coating which gave a higher refractive index as well as a lower dispersion. This resulted in a smaller required curvature of the lenses, hence reducing the cost of production for the lenses [2]. Thorium-232 is a naturally occurring radioactive isotope which marks the beginning of an extensive decay chain that ends with the stable lead-208 [3].

Radioactive radiation may be harmful in too large doses. The effects of such radiation are usually divided into two main categories; deterministic effects and stochastic effects. Deterministic effects will occur if the radiation dose is high enough and increase if the dose is increased and are the result of cell death. The threshold for these effects lies at around 0.1-1 Sv which is higher than expected here. The stochastic effects, on the other hand, are more probabilistic. The probability for stochastic effects increase with a higher dose, but the effects themselves are no more severe and are instead the result of cell mutation whose symptoms may take years to show up. There exists no widely accepted threshold for stochastic effects but recommended dose limits are based upon extensive research on both stochastic and deterministic effects [4].

1.2 Scope

This project will due to financial and material constraints have a restricted area of research. Since we were only able to obtain objectives through the goodwill of camera owner Per-Olof Eriksson this report will restrict itself to smaller cameras.

The scope will also be restricted by the energy range of the used gamma detector. It has an energy range of 3 keV to 10 MeV and hence no data of the radiation outside this spectrum will be measured. However, the expected radiation from the thorium-232 chain will be covered [3], [5].

1.3 Objective

This report aims, primarily, to investigate whether owners of such photographic objectives have any reason to feel anxious about their health. To do this, we will measure gamma radiation from a number of camera lenses, and beta radiation from one lens. The spectra obtained will then be analyzed and the activity of the lenses may then tell us something about the possible health hazards.

2 Materials and Methods

The practical section of the project began with measuring the gamma radiation emanating from the objectives. The objectives were selected through the use of a simple Geiger counter and the measured objectives and corresponding cameras, in the case there is one, are listed in table 1 below. Each camera lens and body in this project was measured for at least 18 hours.

Table 1: The cameras and camera objectives measured in this project.

Cameras	**Objectives**
Nikon F2	Nikkor 50mm 1:2
Contax	Zeiss-Opton Sonnar 50mm 1:1.5
Hasselblad 1000F	Carl Zeiss Tessar 80mm 1:2.8
	Nikkor Vivitar 70-150mm 1:3.8
	Sigma super-wide II 24mm 1:2.8 (multi-coated)
	Nikkor 135mm 1:2.8
	Nikkor-P Auto 105mm 1:2.5
	Lietz-Wetzlar Macro-Elmarit-R 1:2.8/60

Thorium-232 will go through a certain chain of events when decaying, as shown in figure 1.

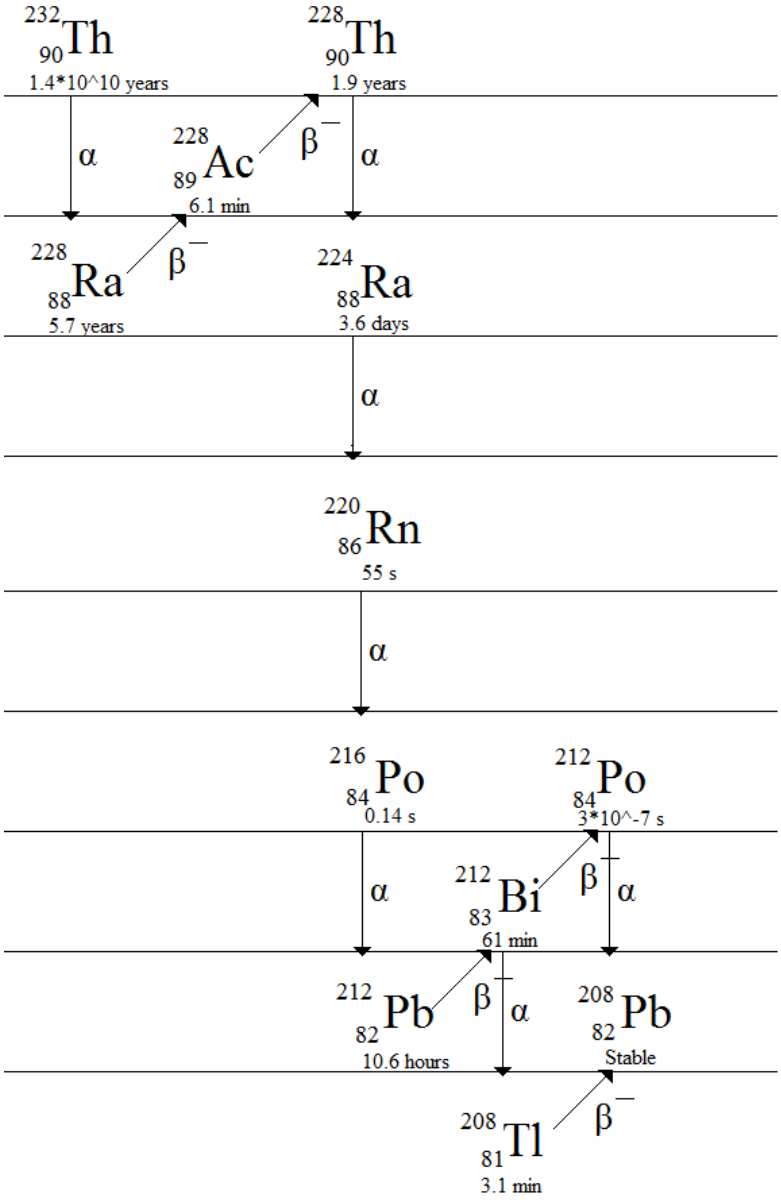

Figure 1: The decay chain originating at Thorium-232 with type of decay and half-time. Data taken from NuDat: National Nuclear Data Center, see reference [3].

In the figure, every isotope completely decays into the following isotope, except for bismuth-212. Since it emits both alpha and beta minus radiation it will create tallium-208 and polonium-212 respectively, which in turn both decay into the stable isotope lead-208. Thorium-232 itself clearly has a substantial half-life and will therefore be present in the lenses for an extensive period of time. The activity of this decay is expected to be rather low in the measurements.

Table 2: The thorium-232 decay chain with some values for the gamma energies radiated from the daughter nucleus in each decay. Data taken from NuDat: National Nuclear Data Center, see reference [3].

Parent nucleus	**Half life**	**Decay mode**	**Q-value [keV]**	**Energy of gamma [keV]**	**Probability of gamma [%]**	**Mean β- energy [keV]**
Thorium-232	$1.4*10^{10}$ years	α: 100%	4082.8	63.81	0.26	-
Radium-228	5.7 years	β-: 100%	45.9	13.52	1.55	7.2
Actinium-228	6.1 minutes	β-: 100%	2127	462.95 911.23 969.03	4.4 25.8 15.8	380
Thorium-228	1.9 years	α: 100%	5520.1	215.98	0.02	-
Radium-224	3.6 days	α: 100%	5788.8	242.1	4.1	-
Radon-220	55 seconds	α: 100%	6404.67	549.73	0.114	-
Polonium-216	0.14 seconds	α: 100%	6906.3	804.9	0.0019	-
Lead-212	10.6 hours	β-: 100%	569.9	238.7 300.2	43.6 3.3	100
Bismuth-212	61 minutes	α: 35.94%	6207.26	10.3	7.0	-
		β-: 64.06%	2252.1	727.26	6.67	771
Polonium-212	$3*10^{-7}$ seconds	α: 100%	8954.12	0	0	-
Thallium-208	3.1 minutes	β-: 100%	4999.0	583.29 860.62 2614.5	85 12.5 99.8	560
Lead-208	Stable	Stable	Stable	Stable	Stable	-

In table 2 above, some of the gamma radiation is shown. The energy and branching ratio of these emissions is seen in column 5 and 6, respectively. This gamma radiation can easily escape from a radioactive sample even if the radioactivity is embedded in the material. The gamma radiation can be detected and the associated activity deduced.

The measurements of gamma radiation were executed using a semiconductor photon detector of the ORTEC-GMX series (model no. GMX40P4-83) with a high-purity germanium crystal. High-purity germanium detectors react with high energy ionizing radiation such as X-rays or gamma rays by producing charge carriers when the material interacts with a high energy photon. These charge carriers are then swept by the electric field inside the detector to the electrodes. The charge is proportional to the interaction energy of the photon and is converted to a voltage pulse by a preamplifier. High purity germanium detectors are characterized by their excellent energy resolution. This is used here to identify the characteristic gamma radiation from different radioactive nuclides. Over time more and more photons will be detected and thereby the energy of the photons can be plotted against the number of counts, leading to an energy spectrum. The spectrum can then be analyzed via a computer program [5], [6].

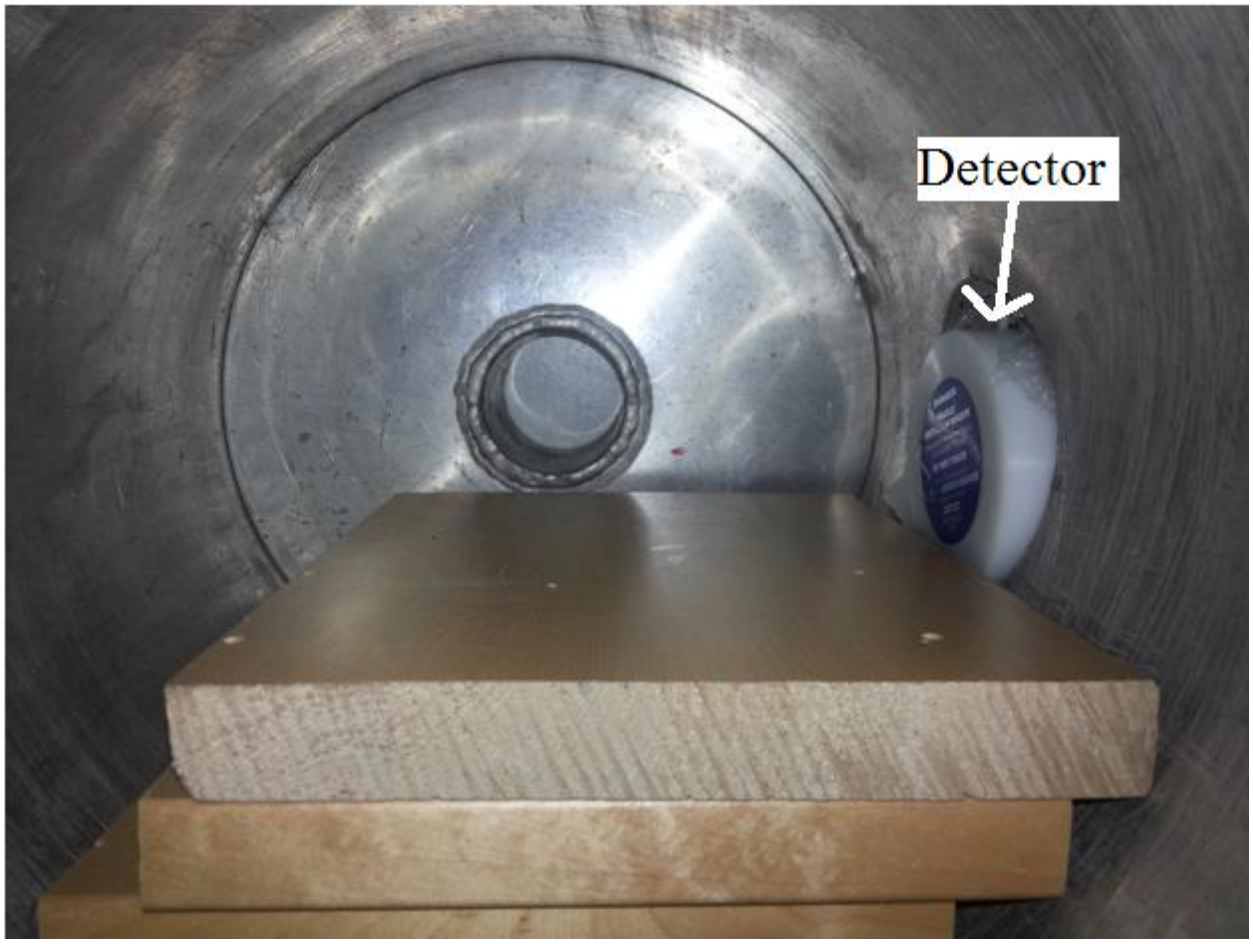

Figure 2: Inside the gamma measurement chamber. The front end of the detector is marked on the right in the image. The walls of the measurement chamber include a 5cm lead layer, shielding against the surrounding natural background gamma ray radiation.

Along with the spectra from objectives and camera bodies, measurements were made of the background radiation. The background radiation was then subtracted from the spectra to give a clear view of the radiation from the lenses. The spectra collected were imported into MATLAB where the intensity was plotted against the energy.

After all the measurements were completed a calibration of the efficiency of the gamma detector had to be made, since radiation emitted by an objective would reach the detector with different probability due to the geometry of the measuring chamber. The detector also has a sensitivity which varies with the gamma ray energy. See Appendix A for full details of the efficiency calibration.

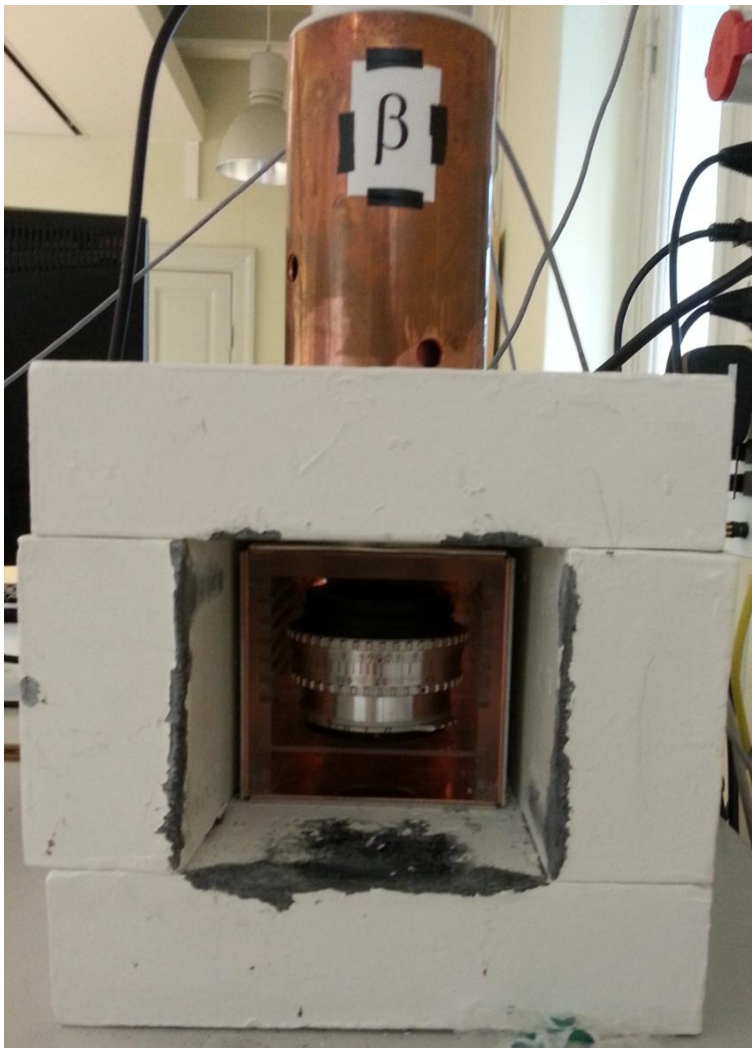

Figure 3: The setup for the beta measurement of the Carl Zess Tessar objective. The measurement chamber consists of 5 cm lead in order to shield from the external background radiation.

Being finished with the measurements of gamma radiation, measurements of the beta radiation would possibly have given a clearer result. Due to time constraints only a measurement on the most promising objective was made; the Carl Zeiss objective belonging to the Hasselblad 1000F camera.

The beta measurements were conducted with a plastic scintillator detector with the grid taken off. A scintillator detector acts on the basis of the material scintillation property when excited by incoming ionizing radiation. The radiation energy is absorbed by the scintillator, which then re-emits the energy in the form of photons which are typically in the visible range. The photons are registered by a photodetector, such as a photomultiplier tube which converts the light pulse into an

amplified electrical signal. The registered radiation may then be displayed as a continuous energy spectrum of beta radiation.

The plastic scintillator used for the measurements had a diameter of 50 mm. It was of a few millimeters thickness and therefore mainly sensitive to charged particles. The setup for the beta measurement is seen in figure 3 above. The lens was placed with the inner side facing the camera towards turned the detector since this was where most radiation was found to be emitted. The lens is also centered to the exact center of the detector at the lowest shelf of the measuring chamber. The lowest shelf was placed 70 mm from the plastic scintillator.

As with the gamma radiation, measurements of the background and the objective were done separately. These were imported to MATLAB for further analysis. An efficiency calibration had to be made for the beta detector as well, but this was done taking only the measurement geometry into account. The full details of the efficiency calibrations are given in Appendix A.

3 Results

The results below are presented as plots of the gamma spectra for the background radiation and a table of the prominent peaks with the corresponding decay for each of the camera objectives and houses. Some plots or tables will also be followed by a brief comment, where fitting. For deeper analysis of the results see section 4; Discussion. Note that the graphs are zoomable when analyzing in the MATLAB software so that some peaks that are in the table may not be visible in the plots as presented in this report. The rows marked with "-" represent values that were disregarded due to high statistical fluctuations.

In the tables for all measurements, except the background, only the decay from the thorium-232 chain will be included since all the other are of little interest to the project. The columns in measurements of both the camera houses and camera objectives are calculated, for each energy according to formulae (1). (2) and (3) below.

$$Measured\ gamma\ intensity\ = \frac{Area\ under\ peak}{Measurement\ time} \quad (1)$$

$$Proportion\ of\ background\ intensity = \frac{Measured\ gamma\ intensity}{Background\ intensity} * 100 \quad (2)$$

$$Total\ isotope\ activity = \frac{Measured\ gamma\ intensity - Background\ intensity}{Efficiency * Gamma\ branching\ ratio} \quad (3)$$

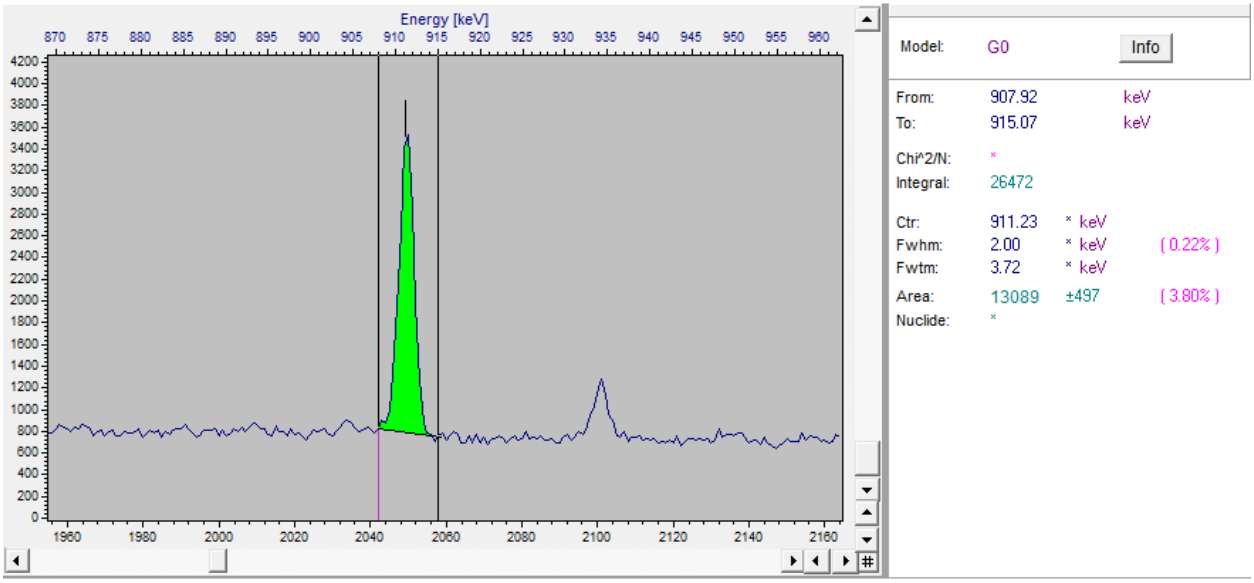

Figure 4: A zoomed peak in the Carl Zeiss Tessar spectrum.

As an example of the analysis, the zoomed peak from the background spectrum as seen in figure 4, above, will be used. The energy of the peak is recorded as well as the area under the peak. The program Tukan 8K will automatically calculate the area under the peak without the background which mainly is due to Compton scattering of higher energy photons. The energy is then compared to values from the National Nuclear Data Center (NuDat) to characterize which decay the peak corresponds to [4]. 911.23 keV is seen to match with the beta minus decay of actinium-228 to thorium-228. The beta decay populates an exited state in thorium-228 and a 911.2 keV photon is then emitted. This is only one out of many characteristic gamma rays from this decay.

The area under the curve is then divided by the live time of the measurement as well as the efficiency of the detector at this energy and the proportion of the decay that is represented by this photon energy. The efficiency is derived from the graph displayed in figure 13 in Appendix A. This will yield the activity of the parent nucleus of the decay in the measured object, in this case actinide-228.

3.1 Background Gamma Radiation

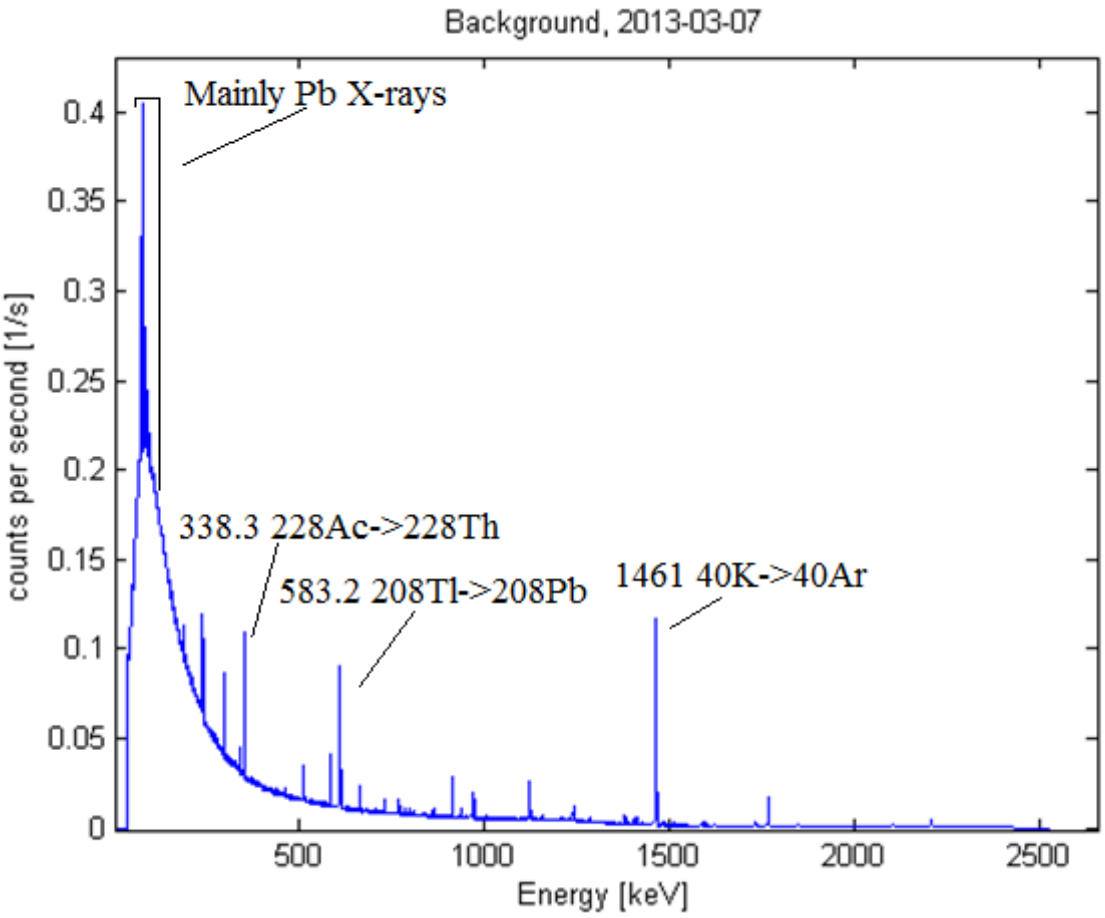

Figure 5: Gamma spectrum of the background radiation measurement.

Table 3: Energy peaks and the corresponding decay for the background radiation.

Nominal energy [keV]	**Decay**	**Populating particle decay mode**	**Relative intensity of gamma[%]**	**Measured intensity [1/s]**
72.873	210Bi->206Tl	alpha	6.30	0.113
74.969	**208Tl->208Pb**	beta-	3.35	0.423
84.214	231Th->231Pa	beta-	6.6	0.244
87.349	**212Pb->212Bi**	beta-	3.97	0.080
93.35	**228Ac->228Th**	beta-	3.1	0.071
185.715	235U->231Th	alpha	57.2	0.068
238.632	**212Pb->212Bi**	beta-	43.6	0.219
240.986	**224Ra->220Rn**	alpha	4.1	0.067
270,245	**228Ac->228Th**	beta-	3.46	0.026
296	210Tl->210Pb	beta-	79	0.214
300.087	**212Pb->212Bi**	beta-	3.3	0.017
338.32	**228Ac->228Th**	beta-	11.27	0.056
351.9321	214Pb->214Bi	beta-	35.6	0.386
463.004	**228Ac->228Th**	beta-	4.4	0.024
510	222Rn->218Po	alpha	0.076	0.127
583.187	**208Tl->208Pb**	beta-	85	0.155
609.32	214Bi->214Po	beta-	45.49	0.449
660.94	214Bi->214Po	beta-	0.053	0.072
727.33	**212Bi->212Po**	beta-	6.67	0.039
768.36	214Bi->214Po	beta-	4.894	0.045
794.947	**228Ac->228Th**	beta-	4.25	0.022
860.557	**208Tl->208Pb**	beta-	12.5	0.025
911.204	**228Ac->228Th**	beta-	25.8	0.147
934.5	214Bi->214Po	beta-	0.01	0.027
965	214Bi->214Po	beta-	0.011	0.023
968.971	**228Ac->228Th**	beta-	15.8	0.081
1120.6	234Pa->234U	beta-	0.00172	0.135
1238.122	214Bi->214Po	beta-	5.834	0.055
1377.669	214Bi->214Po	beta-	3.99	0.035
1460.822	40K -> 40Ar	epsilon	10.66	0.897
1765.44	214Bi->214Po	beta-	15.3	0.133

Table 3, above, shows the background radiation measured in the measuring chamber (see figure 2) of our lab at Alba Nova of the Royal Institute of Technology, Sweden with no source of radiation inside. Notable peaks are the one from potassium-40 and radon-222, radioactive isotopes that are common in Sweden. Some peaks seen here also correspond to decay originating from thorium-232, the decay chain of interest in this thesis, and these are marked with bold letters. If there is indeed radiation from the lenses and camera houses, the

intensities of these will be higher than those derived from Table 3. The energies in the Nominal energy column are taken from [3].

3.2 Camera House Gamma Measurements

3.2.1 Nikon F2

Table 4: Energy peaks from the thorium-232 decay chain for Nikon F2.

Nominal energy [keV]	Decay	Measured gamma intensity [Bq]	Proportion of Background intensity [%]	Efficiency	Total isotope activity [Bq]
87.349	212Pb->212Bi	-	-	-	-
238.632	212Pb->212Bi	0.251	115	0.023	3.20
240.986	224Ra->220Rn	-	-	-	-
338.32	228Ac->228Th	0.062	111	0.017	3.15
583.187	208Tl->208Pb	0.168	109	0.013	1.27
727.33	212Bi->212Po	-	-	-	-
911.204	228Ac->228Th	-	-	-	-
968.971	228Ac->228Th	0.083	103	0.008	1.81

3.2.2 Contax

Table 5: Energy peaks from the thorium-232 decay chain for Contax.

Nominal energy [keV]	Decay	Measured gamma intensity [1/s]	Proportion of Background intensity [%]	Efficiency	Total isotope activity [Bq]
87.349	212Pb->212Bi	-	-	-	-
93.35	228Ac->228Th	-	-	-	-
238.632	212Pb->212Bi	0.278	127	0.023	5.95
240.986	224Ra->220Rn	-	-	-	-
270.245	228Ac->228Th	-	-	-	-
300.087	212Pb->212Bi	-	-	-	-
338.32	228Ac->228Th	0.067	119	0.017	5.50
463.004	228Ac->228Th	-	-	-	-
583.187	208Tl->208Pb	0.185	120	0.013	2.85
727.33	212Bi->212Po	-	-	-	-
794.947	228Ac->228Th	-	-	-	-
860.557	208Tl->208Pb	-	-	-	-
911.204	228Ac->228Th	-	-	-	-
968.971	228Ac->228Th	0.088	109	0.008	5.82

3.2.3 Hasselblad 1000F

Table 6: Energy peaks from the thorium-232 decay chain for Hasselblad 1000F.

Nominal energy [keV]	Decay	Measured gamma intensity [1/s]	Proportion of Background intensity [%]	Efficiency	Total isotope activity [Bq]
87.349	212Pb->212Bi	-	-	-	-
93.35	228Ac->228Th	-	-	-	-
238.632	212Pb->212Bi	0.250	114	0.023	3.15
240.986	224Ra->220Rn	-	-	-	-
270.245	228Ac->228Th	-	-	-	-
300.087	212Pb->212Bi	-	-	-	-
338.32	228Ac->228Th	0.064	113	0.017	3.80
463.004	228Ac->228Th	-	-	-	-
583.187	208Tl->208Pb	0.173	112	0.013	1.75
727.33	212Bi->212Po	0.040	102	0.011	1.50
794.947	228Ac->228Th	-	-	-	-
860.557	208Tl->208Pb	-	-	-	-
911.204	228Ac->228Th	0.157	106	0.009	4.22
968.971	228Ac->228Th	0.086	106	0.008	3.79

3.3 Camera Objective Gamma Measurements

3.3.1 Nikkor 50mm 1:2

Table 7: Energy peaks from the thorium-232 decay chain for Nikkor 50mm 1:2.

Nominal energy [keV]	Decay	Measured gamma intensity [1/s]	Proportion of Background intensity [%]	Efficiency	Total isotope activity [Bq]
87.349	212Pb->212Bi	-	-	-	-
93.35	228Ac->228Th	-	-	-	-
238.632	212Pb->212Bi	0.246	113	0.023	2.75
240.986	224Ra->220Rn	-	-	-	-
270.245	228Ac->228Th	-	-	-	-
300.087	212Pb->212Bi	-	-	-	-
338.32	228Ac->228Th	0.058	104	0.017	1.07
463.004	228Ac->228Th	-	-	-	-
583.187	208Tl->208Pb	0.169	109	0.013	1.34
727.33	212Bi->212Po	-	-	-	-
794.947	228Ac->228Th	-	-	-	-

3.3.2 Zeiss-Opton Sonnar 50mm 1:1.5

Table 8: Energy peaks from the thorium-232 decay chain for Zeiss-Opton Sonnar 50mm 1:1.5.

Nominal energy [keV]	**Decay**	**Measured gamma intensity [1/s]**	**Proportion of Background intensity [%]**	**Efficiency**	**Total isotope activity [Bq]**
87.349	212Pb->212Bi	-	-	-	-
93.35	228Ac->228Th	-	-	-	-
238.632	212Pb->212Bi	0.232	106	0.023	1.26
240.986	224Ra->220Rn	-	-	-	-
270.245	228Ac->228Th	-	-	-	-
300.087	212Pb->212Bi	-	-	-	-
338.32	228Ac->228Th	0.059	105	0.017	1.32
463.004	228Ac->228Th	-	-	-	-
583.187	208Tl->208Pb	0.164	106	0.013	0.91
727.33	212Bi->212Po	-	-	-	-
794.947	228Ac->228Th	-	-	-	-
860.557	208Tl->208Pb	-	-	-	-
911.204	228Ac->228Th	-	-	-	-
968.971	228Ac->228Th	-	-	-	-

3.3.3 Carl Zeiss Tessar 80mm 1:2.8

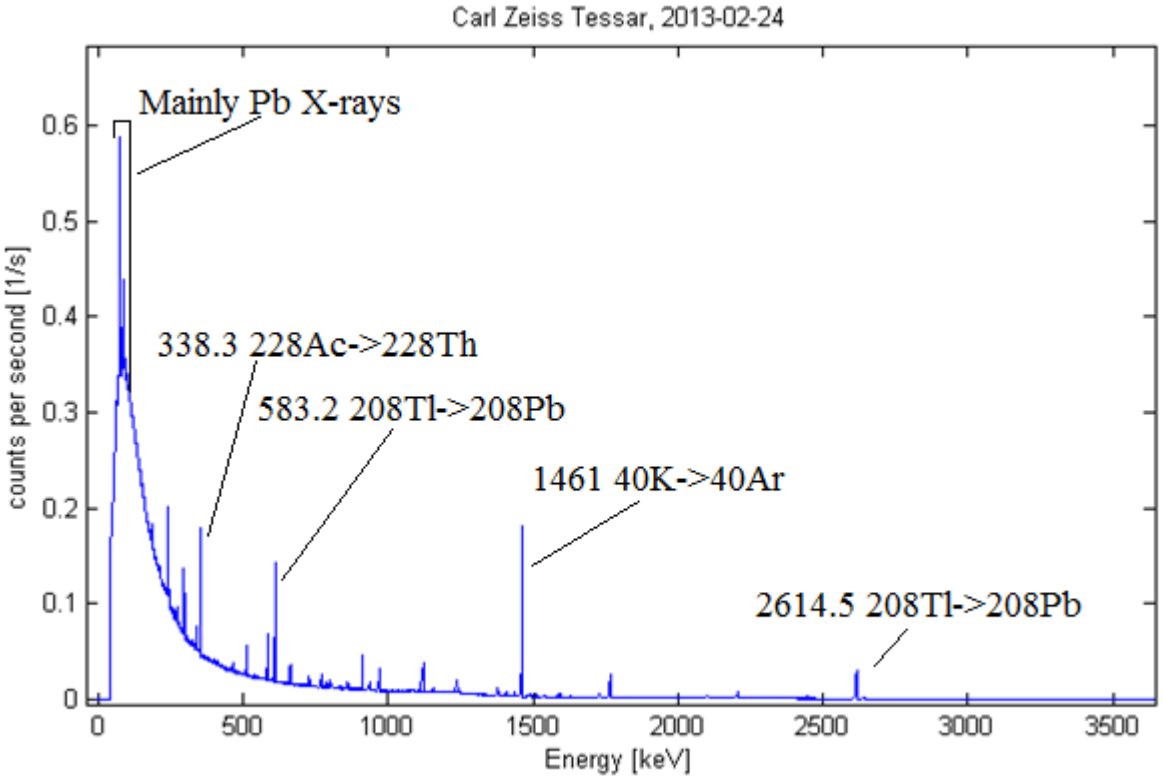

Figure 6: Gamma radiation spectrum for the measurement of the Carl Zeiss Tessar lens.

Table 9: Energy peaks from the thorium-232 decay chain for Carl Zeiss Tessar 80mm 1:2.8.

Nominal energy [keV]	**Decay**	**Measured gamma intensity [1/s]**	**Proportion of Background intensity [%]**	**Efficiency**	**Total isotope activity [Bq]**
87.349	212Pb->212Bi	-	-	-	-
93.35	228Ac->228Th	-	-	-	-
238.632	212Pb->212Bi	0.247	113	0.023	2.78
240.986	224Ra->220Rn	-	-	-	-
270.245	228Ac->228Th	-	-	-	-
300.087	212Pb->212Bi	-	-	-	-
338.32	228Ac->228Th	0.080	142	0.017	12.22
463.004	228Ac->228Th	0.029	122	0.015	8.03
583.187	208Tl->208Pb	0.189	122	0.013	3.16
727.33	212Bi->212Po	0.046	117	0.011	9.37
794.947	228Ac->228Th	0.026	117	0.010	9.21
860.557	208Tl->208Pb	0.028	111	0.009	2.39
911.204	228Ac->228Th	0.168	114	0.009	9.46
968.971	228Ac->228Th	-	-	-	-

In table 9 one can clearly see an increase in the activity from decays in the thorium-232 chain. The actinium-228 decay has several observable gamma radiation peaks that give the total activity of actinium-228. Most of these give similar results.

3.3.4 Nikkor Vivitar 70-150mm 1:3.8

Table 10: Energy peaks from the thorium-232 decay chain for Nikkor Vivitar 70-150mm 1:3.8.

Nominal energy [keV]	**Decay**	**Measured gamma intensity [1/s]**	**Proportion of Background intensity [%]**	**Efficiency**	**Total isotope activity [Bq]**
87.349	212Pb->212Bi	-	-	-	-
93.35	228Ac->228Th	-	-	-	-
238.632	212Pb->212Bi	0.222	102	0.023	0.345
240.986	224Ra->220Rn	-	-	-	-
270.245	228Ac->228Th	-	-	-	-
300.087	212Pb->212Bi	-	-	-	-
338.32	228Ac->228Th	-	-	-	-
463.004	228Ac->228Th	-	-	-	-
583.187	208Tl->208Pb	0.158	102	0.013	0.32
727.33	212Bi->212Po	-	-	-	-
794.947	228Ac->228Th	-	-	-	-
860.557	208Tl->208Pb	-	-	-	-
911.79	228Ac->228Th	-	-	-	-
969.68	228Ac->228Th	-	-	-	-

3.3.5 Sigma super-wide II 24mm 1:2.8 (multi-coated)

Table 11: Energy peaks from the thorium-232 decay chain for Sigma super-wide II 24mm 1:2.8.

Nominal energy [keV]	Decay	Measured gamma intensity [1/s]	Proportion of Background intensity [%]	Efficiency	Total isotope activity [Bq]
87.349	212Pb->212Bi	-	-	-	-
93.35	228Ac->228Th	-	-	-	-
238.632	212Pb->212Bi	0.267	122	0.023	4.81
240.986	224Ra->220Rn	-	-	-	-
270.245	228Ac->228Th	-	-	-	-
300.087	212Pb->212Bi	-	-	-	-
338.32	228Ac->228Th	0.071	127	0.017	7.73
463.004	228Ac->228Th	-	-	-	-
583.187	208Tl->208Pb	0.189	122	0.013	3.23
727.33	212Bi->212Po	-	-	-	-
794.947	228Ac->228Th	-	-	-	-
860.557	208Tl->208Pb	-	-	-	-
911.204	228Ac->228Th	0.161	109	0.009	6.35
968.971	228Ac->228Th	0.092	114	0.008	8.78

3.3.6 Nikkor 135mm 1:2.8

Table 12: Energy peaks from the thorium-232 decay chain for Nikkor 135mm 1:2.8.

Nominal energy [keV]	Decay	Measured gamma intensity [1/s]	Proportion of Background intensity [%]	Efficiency	Total isotope activity [Bq]
87.349	212Pb->212Bi	-	-	-	-
93.35	228Ac->228Th	-	-	-	-
238.632	212Pb->212Bi	0.243	111	0.023	2.43
240.986	224Ra->220Rn	-	-	-	-
270.245	228Ac->228Th	-	-	-	-
300.087	212Pb->212Bi	-	-	-	-
338.32	228Ac->228Th	0.062	110	0.017	2.98
463.004	228Ac->228Th	-	-	-	-
583.187	208Tl->208Pb	0.189	122	0.013	3.19
727.33	212Bi->212Po	-	-	-	-
794.947	228Ac->228Th	-	-	-	-
860.557	208Tl->208Pb	-	-	-	-
911.204	228Ac->228Th	0.158	107	0.009	4.89
968.971	228Ac->228Th	0.089	111	0.008	6.72

3.3.7 Nikkor-P Auto 105mm 1:2.5

Table 13: Energy peaks from the thorium-232 decay chain for Nikkor-P Auto 105mm 1:2.5.

Nominal energy [keV]	Decay	Measured gamma intensity [1/s]	Proportion of Background intensity [%]	Efficiency	Total isotope activity [Bq]
87.349	212Pb->212Bi	-	-	-	-
93.35	228Ac->228Th	-	-	-	-
238.632	212Pb->212Bi	0.132	117	0.023	3.75
240.986	224Ra->220Rn	-	-	-	-
270.245	228Ac->228Th	-	-	-	-
300.087	212Pb->212Bi	-	-	-	-
338.32	228Ac->228Th	0.049	122	0.017	6.23
463.004	228Ac->228Th	-	-	-	-
583.187	208Tl->208Pb	0.046	121	0.013	3.01
727.33	212Bi->212Po	0.016	112	0.011	6.73
794.947	228Ac->228Th	-	-	-	-
860.557	208Tl->208Pb	-	-	-	-
911.204	228Ac->228Th	-	-	-	-

3.3.8 Lietz-Wetzlar Macro-Elmarit-R 1:2.8/60

Table 14: Energy peaks from the thorium-232 decay chain for Leitz-Wetzlar Macro-Elmarit-R 1:2.8/60

Nominal energy [keV]	Decay	Measured gamma activity [Bq]	Proportion of Background intensity [%]	Efficiency	Total isotope activity [Bq]
87.349	212Pb->212Bi	-	-	-	-
93.35	228Ac->228Th	-	-	-	-
238.632	212Pb->212Bi	0.260	119	0.023	4.13
240.986	224Ra->220Rn	-	-	-	-
270.245	228Ac->228Th	-	-	-	-
300.087	212Pb->212Bi	-	-	-	-
338.32	228Ac->228Th	0.063	111	0.017	3.27
463.004	228Ac->228Th	-	-	-	-
583.187	208Tl->208Pb	0.179	116	0.013	2.27
727.33	212Bi->212Po	0.046	117	0.011	9.35
794.947	228Ac->228Th	-	-	-	-
860.557	208Tl->208Pb	-	-	-	-
911.204	228Ac->228Th	0.156	106	0.009	4.07
968.971	228Ac->228Th	-	-	-	-

3.4 Beta Measurements

Due to a shortage of time, only one measurement of beta radiation was made in addition to the background radiation, a measurement of the Carl-Zeiss Tessar objective. This objective showed the largest enhancement in activity over the background in gamma ray measurements.

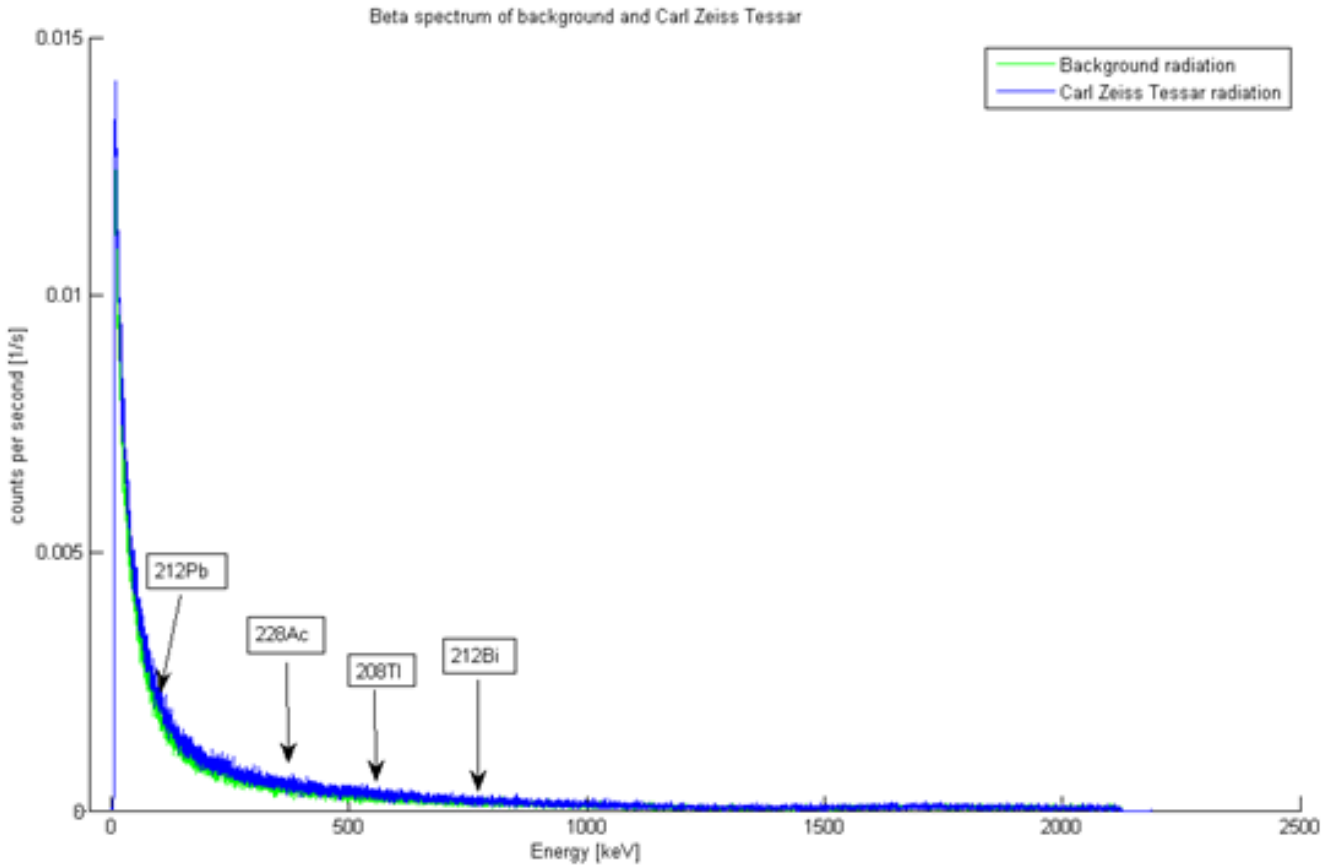

Figure 7: Beta spectrum of both the background (green) and objective (blue). The mean beta energy per decay of most isotopes in the thorium-232 decay chain are indicated.

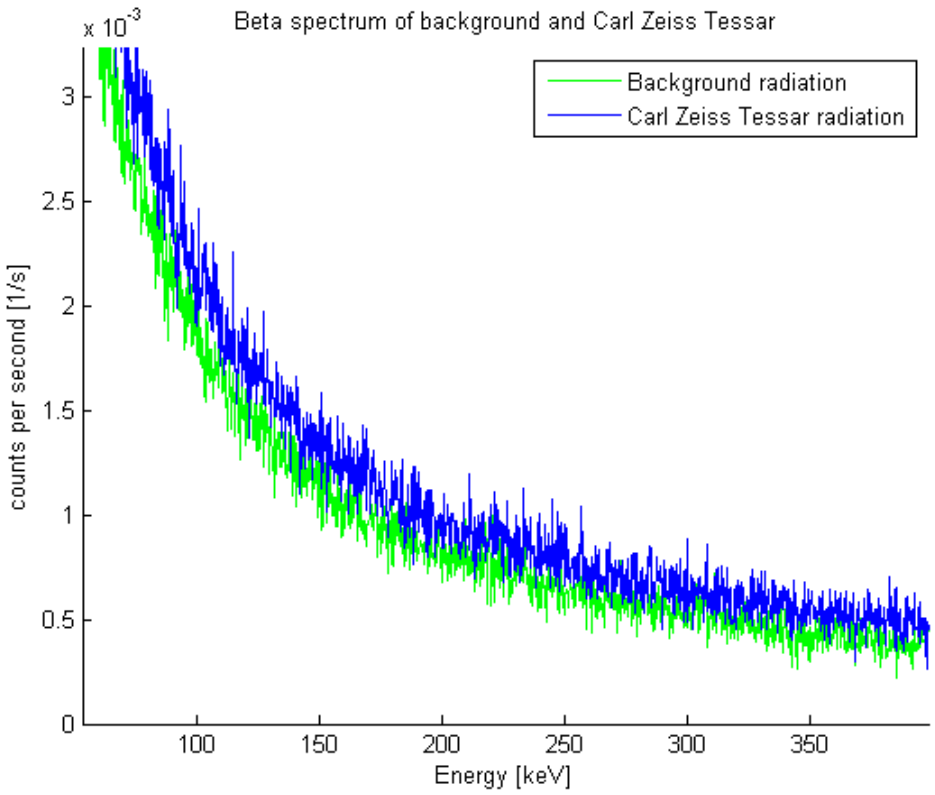

Figure 8: Zoomed image of the beta spectrum.

In the spectrum of beta radiation separate peaks cannot be isolated; it is a continuous spectrum. Instead of observing specific decays, the whole activity is therefore calculated by integrating the entire spectrum.

As with the gamma radiation Tukan 8k is used to get a total area below the spectrum to yield the total number of counts from which the number of counts from the background is subtracted. This is then divided by the time measured and the absolute efficiency of the beta detector to yield the results in table 15.

Table 15: The measured activity of the beta radiation for the Carl Zeiss Tessar lens.

Background intensity [1/s]	**Measured intensity of Carl Zeiss Tessar [1/s]**	**Efficiency**	**Total beta activity [Bq]**
3.19	3.71	0.098	5.41

4 Discussion

From the gamma spectra, it is clear that most camera objectives and the camera houses rarely give higher intensities than 115% of the background radiation. Since a simple Geiger meter was used to assist the choosing of which objectives to measure more precisely, no objectives were chosen that gave off little or no radiation. Thereby, the increase in activity - however slight - observed on all measurements was expected.

The objective measurement that gave the most significant activity increase was the Carl Zeiss Tessar with most discernible peaks from the thorium-232 chain and an average gamma ray enhancement over the background intensity of around 20%. Since the aim of the thesis is to see whether or not thoriated camera lenses pose a health hazard, this case is of major interest. Therefore, the Carl Zeiss Tessar will serve as the main study for the remainder of this report.

4.1 Activity of the Carl Zeiss Tessar Lens

The Hasselblad 1000F camera was introduced on the market in the 1953 [7]. Since the Carl Zeiss Tessar that was measured was originally mounted on this camera model, it is safe to assume that the lens was manufactured around the same time, or a few years after. The assumption is made that the Tessar objective was manufactured 55 years ago and that, since thorium-232 has such a long half life ($1.4*10^{10}$ years) it can be considered an inexhaustible reservoir. By assuming that thorium-232 has an arbitrary starting activity it is possible to calculate the percentage activities of the rest of the decays in the thorium-232 chain, knowing their half lives. This calculation was done through a simple simulation using the formulas below.

$$A_n = N_0 \sum_{i=1}^{n} c_i e^{-\lambda_i t} \tag{4}$$

$$c_m = \frac{\prod_{i=1}^{n} \lambda_i}{\prod_{i=1}^{n} (\lambda_i - \lambda_m)} \tag{5}$$

Where A_n is the activity for the n:th nuclide in the decay chain, and λ_i is the decay constant for nuclide i in the decay chain. Note that $i \neq m$ in the denominator of (5). The resulting activity ratio is shown in table 16 below together with the activities measured in this thesis.

Table 16: Table of the measurement results as well as calculated activity ratios

Parent nucleus	Half life	Activity Ratio [%]	Activity from gamma measurements [Bq]	Mean activity [Bq]
Th-232	$1.4*10^{10}$ years	100.00	-	9.56
Ra-228	5.7 years	99.87	-	9.55
Ac-228	6.1 minutes	99.87	9.73	9.55
Th-228	1.9 years	99.80	-	9.55
Ra-224	3.6 days	99.80	-	9.55
Rn-220	55 seconds	99.80	-	9.55
Po-216	0.14 seconds	99.80	-	9.55
Pb-212	10.6 hours	99.80	-	9.55
Bi-212	61 minutes	99.80	9.37	9.55
Po-212	3*10^(-7) seconds	63.94	-	6.12
Tl-208	3.1 minutes	35.86	2.78	3.43

The activity from gamma has been calculated through a mean of the values from table 9. Here, some values have been disregarded due to a large discrepancy from the other values. The discrepancy could be explained by the fact that other decays radiate gamma of around this energy, resulting in a larger intensity than the actual intensity of the specific decay of interest. The low energy level discrepancies can also be explained by the fact that the measuring chamber is made of lead. The lead can then be activated by a radioactive sample in the chamber, resulting in lead X-rays. These are prominent in the low energy range of the spectrum. The mean activity is calculated using the activity ratio, given from the simulation described earlier, and the measured values of the activity for actinium-228 and bismuth-212.

The activities seem to correlate quite closely to the calculated ratio. It is also noticeable how the activity ratios correspond to the half lives of the parent nuclei. For example, radium-228 acts as a bottle neck, but when it finally decays the following isotopes decay very rapidly. The last two values arise since bismuth-212 decays both with alpha and beta decay. The ratios of these decays (as seen in table 2) correspond perfectly to the values in table 16. The total activity of the Carl Zeiss Tessar is calculated, from this, to be 96 Bq.

It is also very interesting to compare the total beta decay radiation from the gamma measurements to the beta measurements. By summing up the activities of the beta decays in table 19, it is calculated that the gamma radiations give a total beta activity in the Tessar lens of 38.2 Bq whereas the beta measurement only gave 5.4 Bq. The large difference could, partially, be explained by the purely geometrical

beta detector efficiency calibration resulting in an overestimation of the efficiency. A second explanation is the fact that most Q-values for decays in the thorium-232 chain lay outside the range of the beta detector. Yet a third reason is given by the cut-off that the beta detector makes at low energy levels. The result from the gamma radiation experiment is therefore regarded more precise.

4.2 Radiation Dose from the Carl Zeiss Tessar

With the activity of the lens established, it is desirable to calculate the radiation dose a photographer would absorb while using the Carl Zeiss Tessar objective. This will possibly illuminate the radiation related hazards involved with the lens. In order to do this, the first thing to do is to go over the radiation dose limits set by the Swedish Radiation Protection Authority. This will give values to compare the results to. The yearly maximum effective dose for a person not working with radioactive materials is 1 mSv [9]. If the radiation is incident on the eye's lens, however, the limit is set at 15 mSv equivalent dose [9]. Beta radiation is stopped much easier than gamma since beta radiation interacts with other particles quite readily, much more frequently than gamma particles. Therefore, one can assume that the beta radiation will be incident on the user's eye whereas the gamma radiation will instead be evenly absorbed by the user's body.

The mean beta energy in table 2 shows, for each beta decay in the thorium-232 decay chain, the mean beta energy radiated per decay. This yields, for the beta activities deduced in the gamma measurements, a total mean beta energy per second of 14 MeV/s, which is equal to $2.2*10^{-12}$ J/s, for the entire thorium-232 decay chain.

Assuming that a photographer works for 240 days per year and that he has the camera held towards his face for one hour every day, his eye would be exposed to the beta radiation for 240 hours per year. The radiation does not all go directly into the eye, but rather is emitted evenly in a sphere around the camera lens. By assuming that the eyes lens has a diameter of 10 mm and that the camera lens is located 150 mm away from the eye, it can be calculated that around $\frac{1}{3600}$ of the beta radiation reaches the eye. The mass of an eyes lens, L (in mg), can be calculated by the use of formula (6) below [10].

$$L = 1.32 * A + 141 \quad (6)$$

Here, A is the age of the person. An average professional photographer is assumed to be of age 40. This gives a mass of the eye's lens as 193 mg. This would give an annual absorbed dose, D_β, according to formula (7).

$$D_\beta = \frac{2.23*10^{-12}\ \mathrm{J/s}}{193*10^{-6}\mathrm{kg}} * \frac{1}{3600} * (240 * 3600)\ \mathrm{s} = 2.77\ \mu\mathrm{Gy} \quad (7)$$

To be able to compare this to the maximum dose set by the Swedish Radiation Protection Authority (15 mSv/year), the absorbed dose must first be converted to the equivalent dose, $H_{\mathrm{T},\beta}$. This is done using the formula below.

$$H_{T,\beta} = W_{R,\beta} * D_\beta \quad (8)$$

Here, $W_{R,\beta}$is the radiation weighting factor which is equal to 1 for electrons. Therefore, 2.77 μGy absorbed dose translates to 2.77 μSv equivalent dose. From this, it is seen that the contribution to the annual maximum radiation dose to the eye's lens from this camera lens is 0.2 ‰.This is indeed a contribution, but a very insignificant one. This amount of usage of the Carl Zeiss Tessar lens is therefore deemed non hazardous in terms of beta radiation.

The gamma radiation absorbed by a photographer is equally interesting. By observing the intensity of gamma rays at different energy levels emitted from a certain decay, a mean gamma energy per decay is found [3].

Table 17: Table of the gamma energy released from the decays in the thorium-232 chain for the Carl Zeiss Tessar.

Parent nucleus	**Mean activity[Bq]**	**Mean total gamma energy released [keV/decay]**	**Emitted gamma power [keV/s]**
Th-232	9.56	14.5	139
Ra-228	9.55	13.2	126
Ac-228	9.55	478	4570
Th-228	9.55	27.3	261
Ra-224	9.55	216	201
Rn-220	9.55	550	5250
Po-216	9.55	805	7680
Pb-212	9.55	154	1470
Bi-212	9.55	561	5350
Po-212	6.11	0.00	0.00
Tl-208	3.43	1480	5070

By adding the emitted gamma power a total energy release of the thorium-232 chain for the Carl Zeiss Tessar is found to be 32 MeV/s which is equal to $5*10^{-12}$ J/s. Since gamma radiation is not shielded by the camera itself, a photographer using the Carl Zeiss Tessar would receive gamma radiation to the whole torso whilst carrying the camera. The assumption is made that an average photographer carries his camera for all eight hours of his working days. One third of the gamma radiation is assumed to be absorbed by the whole body of the photographer who has a mass of 70 kg. The absorbed dose, D_γ, is then calculated by the following formula.

$$D_\gamma = \frac{5*10^{-12}\text{J/s}}{70\text{ kg}} * \frac{1}{3} * (240 * 8 * 3600)\text{ s} = 0.17\ \mu\text{Gy} \quad (9)$$

This is converted to effective dose, $H_{E,\gamma}$, according to formula (10).

$$H_{E,\gamma} = \sum_T W_T * H_{T,\gamma} \quad (10)$$

In this case, the whole body is irradiated, meaning that the tissiue weighting factor, W_T, is equal to 1. $H_{T,\gamma}$ is given using the same calculation as in formula (9) with $W_{R,\gamma} = 1$. This gives an effective dose from gamma radiation from the Carl Zeiss Tessar lens on the whole body of the photographer of 0.17 μSv. This, compared to the standards set by the Swedish Radiation Protection Authority, is only 0.17‰ of the maximum allowed dose.

4.3 Error Analysis

The systematic errors of the measurements done in this project consisted mainly of the efficiency calibrations. All of the measurements for the efficiency calibration of the gamma detector displayed large amount of pile-up. Therefore, the geometrical efficiency had to be extrapolated from the best point of measurement. This means that the efficiency of the gamma detector may very well differ from the result in this report. The efficiency calibration of the beta detector was done purely geometrical. The lens was assumed to radiate as a point source located at the center of the objective which, of course, is inaccurate. This means that the distances from the edges of the objective were unaccounted for. The intrinsic efficiency of the detector itself was also assumed to be perfect. These assumptions ultimately result in an overestimated efficiency of the beta detector.

The absolute error of the calculated areas, σ, (as described in the beginning of section 3: Results) propagates through all calculations according to the error propagation formulae.

This error analysis has only been done for the Carl Zeiss Tessar since this objective has been the focus of the rest of the discussion. The table below shows the result of this error analysis.

Table 18: The original area errors and the resulting error for total isotope activity for the Carl Zeiss Tessar

Parent nuclide	Nominal energy [keV]	Absolute area error for the Carl Zeiss Tessar peaks.	Absolute area error for the background peaks.	Absolute total isotope activity error [Bq]
212Pb	238.632	770	823	1.38
228Ac	338.32	609	560	5.25
228Ac	463.004	412	445	11.5
208Tl	583.187	451	488	0.76
212Bi	727.33	324	410	9.00
228Ac	794.947	272	356	13.2
208Tl	860.557	284	338	4.76
228Ac	911.204	383	466	3.32

This generates, through the continued use of the error propagation formulae, an absolute error for the total activity of the Carl Zeiss Tessar of 10.5 Bq. The propagation of the errors is highly noticeable since the resulting errors are obviously very high, even though only areas with relative errors below 10 % were used.

5 Summary and Conclusions

Gamma radiation measurements were made on eight different camera lenses and three camera houses. The gamma spectra produced showed that most lenses and, indeed, also camera houses had some radioactive activity. One camera lens, the Carl Zeiss Tessar, stood out amongst the rest with a higher activity. A complementary beta radiation measurement was conducted on this lens. Efficiency calibrations were made on both detectors to give the efficiency curve, shown in figure 7, for the gamma detector and an efficiency value of 9.8% for the beta detector.

The total measured activity of the Carl Zeiss Tessar lens was measured to be 96 ± 10 Bq. The total beta energy released per second from the thorium-232 decay chain from the Carl Zeiss Tessar objective was about 14 MeV/s. This would give a contribution to the maximum annual radiation dose of the eye's lens, set by the Swedish Radiation Protection Authority for a person not working with radioactive materials, of merely 0.2 ‰ for an average professional photographer.

The total gamma energy released every second from the Carl Zeiss Tessar, on the other hand, was almost 32 MeV/s. The contribution from this for a photographer to the maximum annual dose to the whole body was calculated to be just 0.17 ‰. This is comparable to the increased dose from beta radiation. Thereby the beta and gamma radiation from the Carl Zeiss Tessar are equally non hazardous.

These ratios are so close to zero that the conclusion drawn in this thesis is that there are no radiation related health hazards involved in the usage of any of the camera lenses measured.

Bibliography

[1] Paul F. De Paolis Optical Glass, US Patent 2,466,392
[2] *Thoriated Camera Lens (ca.1970s)*. (Last updated: 2001-09-24) Available: http://www.orau.org/ptp/collection/consumer%20products/cameralens.htm [2013-04-23]
[3] *National Nuclear Data Center* Available: http://www.nndc.bnl.gov/nudat2/ [2013-04-12]
[4] *Radiation Safety Information* Avalible: http://www.nuclear.kth.se/courses/lab/latex/radsafe.pdf [2013-05-16]
[5] *GMX Series Coaxial HPGe Detector Product Configuration Guide* Available: http://www.ortec-online.com/download/gamma-x.pdf [2013-04-23]
[6] *Germanium Detectors* Available: http://www.canberra.com/products/detectors/pdf/Germanium-Det-SS-C36151.pdf [2013-04-23]
[7] *Hasselblad 1000F Instruction Book* Avalible: http://hasselbladhistorical.eu/PDF/Brochures/1000F_Man.pdf [2013-05-19]
[8] What types of radiation are there?, Avalible: http://hps.org/publicinformation/ate/faqs/radiationtypes.html [2013-05-10]
[9] Swedish Radiation Safety Act (Strålskyddslagen), SFS 1988:220
[10] Spencer, RP. (1976). Change in Weight of the Human Lens with Age. Annals of Ophthalmology, Apr;8(4), 440-1.

6 Appendix A: Efficiency Calibration

The efficiency calibration was done by placing four known sources of radiation (americium-241, barium-133, cesium-137 and cobalt-60) at five different points in the chamber. These are marked with red crosses in figure 9. The points were chosen to represent the geometry of the investigated objectives and camera bodies and the radioactive samples were chosen to cover the energy range of interest for the thorium-232 decay chain. Then, the measured activity in each point was compared with the nominal activity of the calibration sources. In this way, the measured efficiency curve should represent both intrinsic and geometrical efficiency.

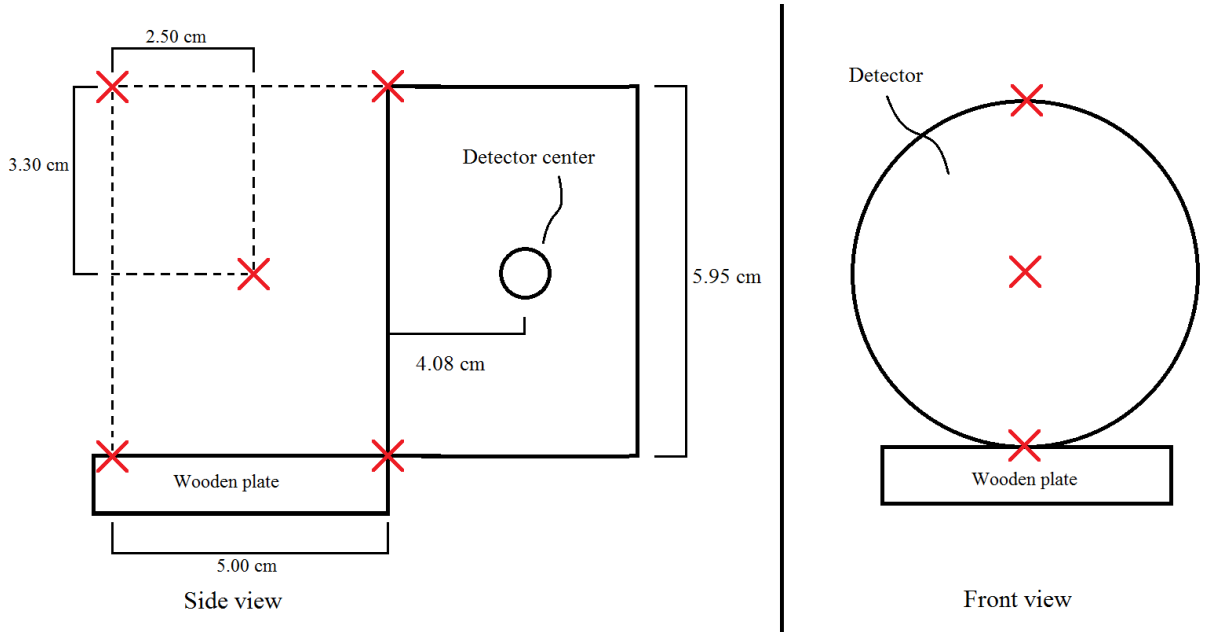

Figure 9: The points of measurement in the chamber for the efficiency calibration. Compare to figure 2.

For the gamma detector, the four control samples had their activity measured on the 1st of October, 1988, and the calibration took place on 11th of April, 2013, giving a discrepancy of 8 957 days.
The current activity is calculated as

$$A = A_0 e^{-\ln(2)*\frac{t}{T_{1/2}}} \quad (11)$$

where $T_{1/2}$ is the half-life in days, and t = 8 957 days. This yields the results presented in Table 19 below.

Table 19: The activity of the control samples.

Sample	Half-life (days)	Initial activity (kBq)	Current activity (kBq)
Americium-241	153004	463.98	446
Barium-133	3838.7	387.02	77.3
Cesium-137	11019	391.46	222.84
Cobalt-60	1925.2	401.82	15.99

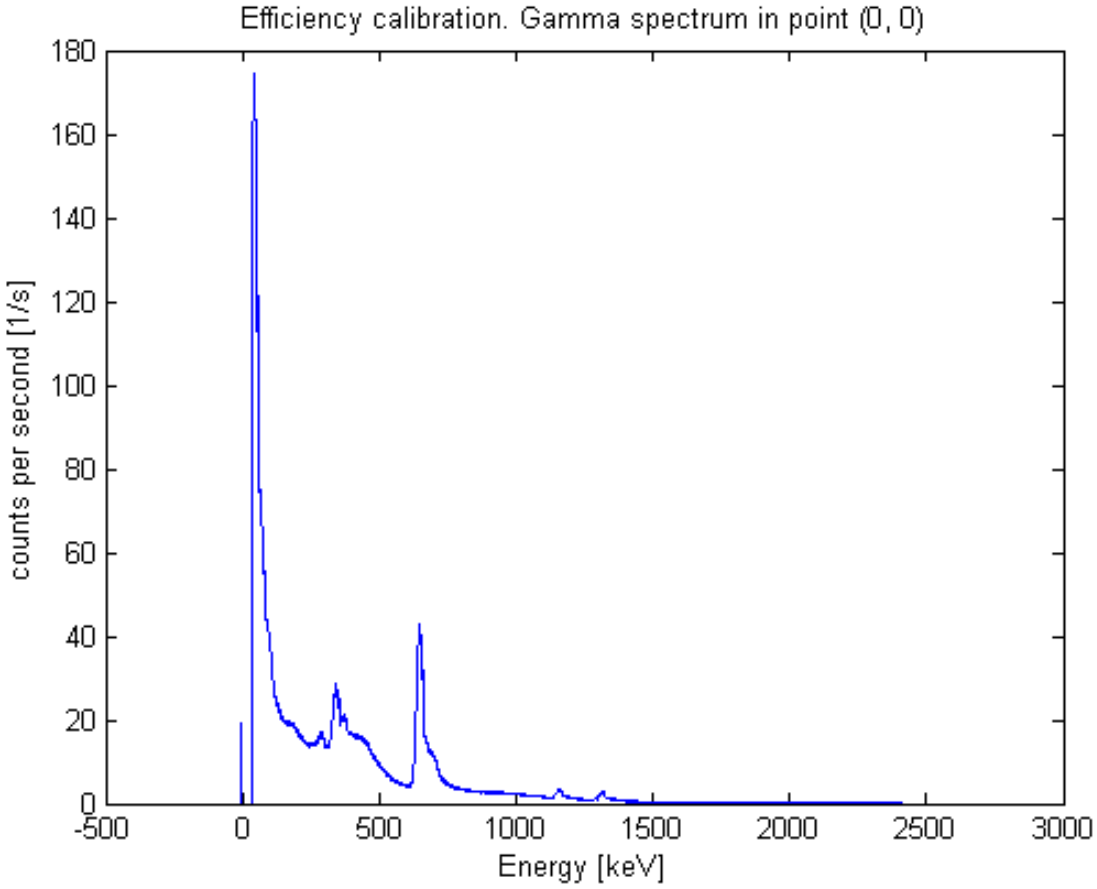

Figure 10: Spectrum of gamma radiation from control samples in point (0,0).

Figure 10, above, shows the measured radiation in point (0, 0), as displayed in figure 9, during the efficiency calibration. This spectrum displays massive amounts of pile-up. Pile-up refers to when too much radiation is incident on the detector for it to handle resulting in the wider type of peaks seen in the plot. This renders the values from this measuring point to be useless.

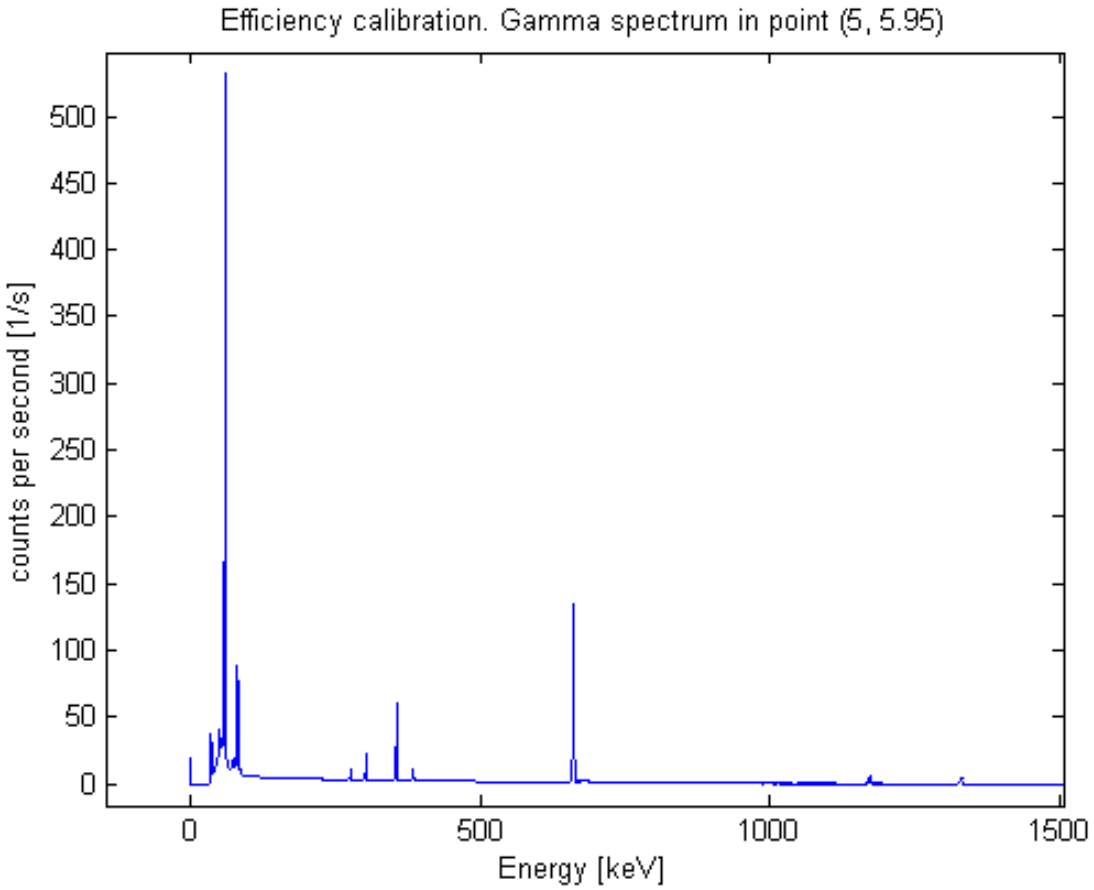

Figure 11: Spectrum of gamma radiation from control samples in point (5, 5.95).

All points exhibited pile-up, but the point (5, 5.95) had the best spectrum in terms of the least pile up. This spectrum is shown in figure 11, above. Therefore this plot was used in the calculations of the detectors efficiency. By comparing the measured activity for different energy levels with the calculated activity in table 19 above, the efficiencies in point (5, 5.95), as shown in figure 9, are calculated for different energy levels.

By assuming the geometrical efficiency to be dependent on the distance to the detector crystal squared, the geometry was accounted for by calculating the efficiency for different energy levels in the remaining points. Figure 3 displays the distances from all points to the center of the detector which are used in formula (12) below.

$$\varepsilon_{tot} = \varepsilon_{(5,5.95)} * r_{(5,5.95)}^2 * < \frac{1}{r^2} > \quad (12)$$

Here, ε_{tot} is the total efficiency of the detector, with geometry accounted for, $r_{(5,5.95)}$ is the distance from point (5, 5.95) to the center of the detector and $< \frac{1}{r^2} >$ is the mean value of the inverse squared distances from all points to the detector center. From this a mean value of efficiency for all points could be calculated and a cubic spline was then fitted to this data.

Table 20: Energy peaks from control samples, point (5, 5.95).

Experimental Energy [keV]	**Decay**	**Measured gamma intensity [1/s]**	**Intensity [%]**	**Total activity [Bq]**	**Nominal activity [kBq]**	**Efficiency**
59.54	241Am -> 273Np	174.6	35.9	485.84	446	0.00110
80.9979	133Ba -> 133Cs	121.2	32.9	367.74	77.3	0.00480
302.8508	133Ba -> 133Cs	17.08	18.34	92.92	77.3	0.00121
356.0129	133Ba -> 133Cs	28.5	62.05	45.76	77.3	0.000597
383.8485	133Ba -> 133Cs	21.25	8.94	237.41	77.3	0.00310
661.657	137Cs -> 137Ba	42.89	85.1	50.37	222.84	0.00220
1173.23	60Co -> 60Ni	3.424	99.85	3.42	15.99	0.000214
1332.492	60Co -> 60Ni	2.723	99.9826	2.72	15.99	0.00017

Table 21: The mean value of efficiency at different energies for the gamma detector.

Energy Level [keV]	Efficiency at point (0, 0)	Efficiency at point (0, 5.95)	Efficiency at point (5, 0)	Efficiency at point (2.5, 3.3)	Efficiency at point (5, 5.95)	Efficiency Mean Value
59.54	0.05719	0.05719	0.00110	0.03369	0.00110	0.00329
80.9979	0.05637	0.05637	0.00480	0.03320	0.00480	0.00431
302.8508	0.02941	0.02941	0.00121	0.01732	0.00121	0.00180
356.0129	0.02685	0.02685	0.00060	0.01582	0.00060	0.00132
383.8485	0.01811	0.01811	0.00310	0.01067	0.00310	0.00242
661.657	0.01068	0.01068	0.00220	0.00629	0.00220	0.00721
1173.23	0.00964	0.00964	0.00021	0.00568	0.00021	0.00040
1332.492	0.05719	0.05719	0.00017	0.03369	0.00017	0.00033

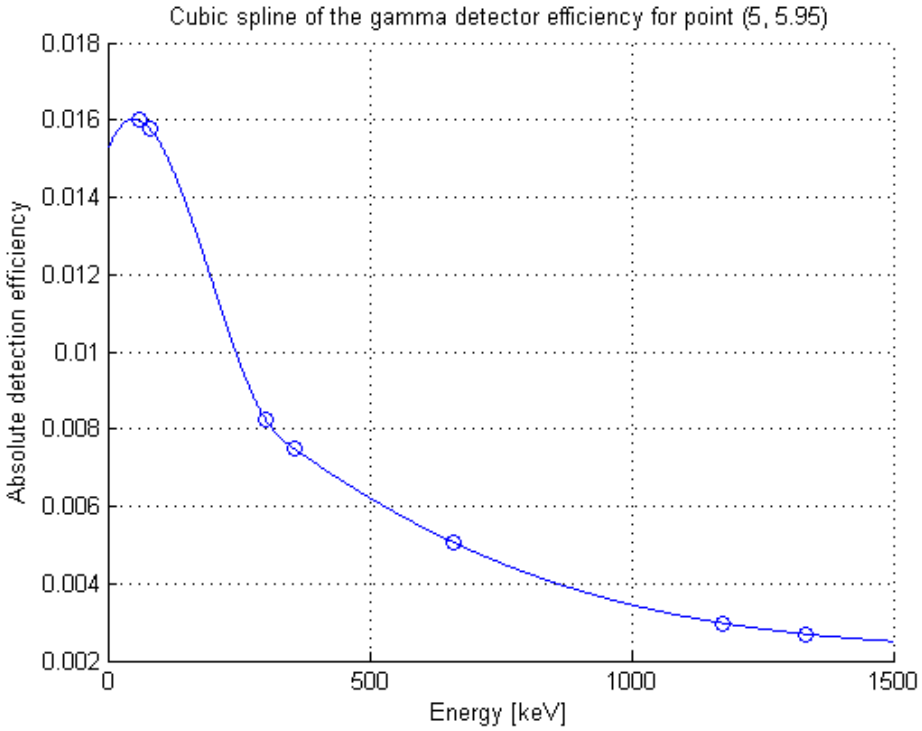

Figure 12: Cubic spline of the gamma detector efficiency over our energy interval for point (5, 5.95)

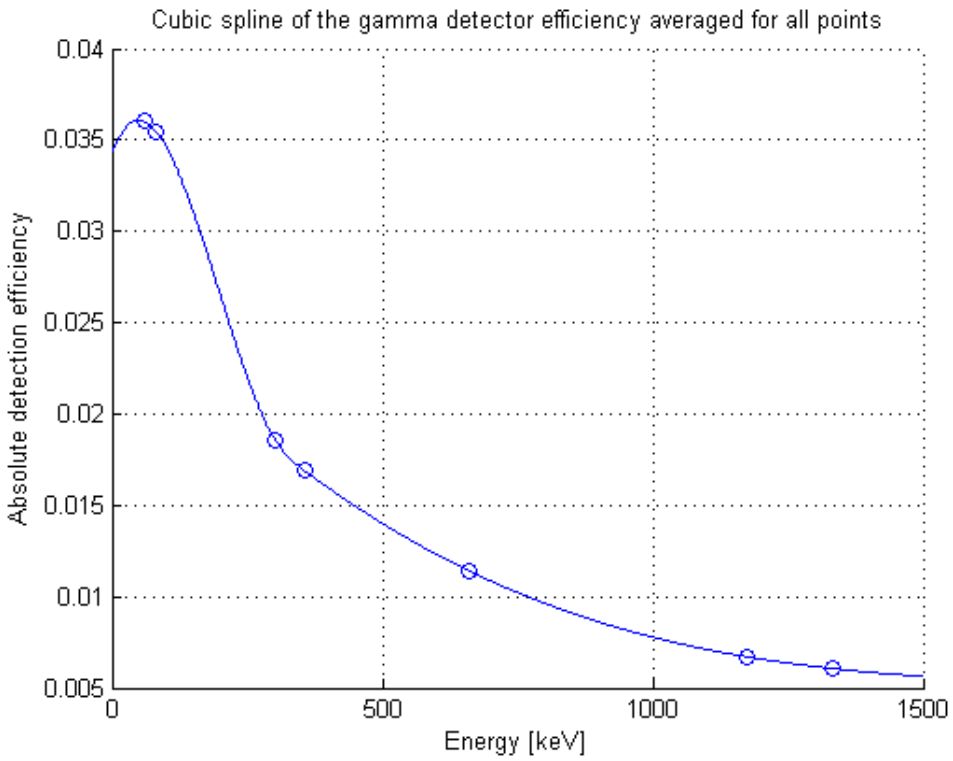

Figure 13: Cubic spline of the gamma detector efficiency over our energy interval with geometry accounted for.

For the beta detector, the assumption is made that the detector itself is 100% efficient given that a beta particle is incident on the detector. The plastic scintillator has a diameter of 50 mm, giving an area of $1.96 * 10^{-3}$ m^2. The lens was placed on the lowest shelf of the chamber which was 70 mm from the detector, as seen in figure 3. The lens itself was 50 mm high. Assuming that the lens radiates as a point source located at the center of the lens, and that this point source radiates evenly in all directions the geometrical efficiency of the detector will then be the ratio of the area of the detector and the area of the sphere with center at the point source and radius as the distance between the point source and the detector.

$$\frac{Area_{detector}}{Area_{radiation\ sphere}} = \frac{\pi(0.025\ \mathrm{m})^2}{4\pi\left(0.070\ \mathrm{m} - \frac{0.060}{2}\ \mathrm{m}\right)^2} = 0.098 \qquad (13)$$

The efficiency of the beta detector is thereby 9.8% with this setup. The uncertainty of this value is of the order of a few percent.